


## Statistical Mechanics of Low Angle Grain Boundaries in Two Dimensions

Grace H. Zhang  and David R. Nelson*Department of Physics, Harvard University, Cambridge, Massachusetts 02138, USA* (Received 7 September 2020; revised 17 October 2020; accepted 23 October 2020; published 20 November 2020)

We explore order in low angle grain boundaries (LAGBs) embedded in a two-dimensional crystal at thermal equilibrium. Symmetric LAGBs subject to a Peierls potential undergo, with increasing temperatures, a thermal depinning transition; above which, the LAGB exhibits transverse fluctuations that grow logarithmically with interdislocation distance. Longitudinal fluctuations lead to a series of melting transitions marked by the sequential disappearance of diverging algebraic Bragg peaks with universal critical exponents. Aspects of our theory are checked by a mapping onto random matrix theory.

DOI: [10.1103/PhysRevLett.125.215503](https://doi.org/10.1103/PhysRevLett.125.215503)

Grain boundaries, which are interfaces dividing crystal grains with distinct orientations, significantly impact the properties of all polycrystalline materials [1–3]. Their dynamics directly affect grain growth stagnation [4], grain boundary mobility [5], superplasticity [6], and shear strength [7,8], altering the microstructure evolution of a wide class of materials [3], including high- $T_c$  superconductors [9] and two-dimensional (2D) materials [10–12]. A complete understanding of grain boundary dynamics is crucial for informing materials synthesis methods and industrial processes [3,13–15].

While previous works have focused on the roughening [16–20], defaceting [5,21], premelting [22,23], and structural phase transitions [24,25] in three-dimensional crystals, recent advances in colloid science [26] and 2D electronic devices [27–29] have triggered studies of grain boundaries in 2D crystals, with electronic and thermal properties especially sensitive to lattice imperfections [30–38].

In two dimensions, grain boundaries have been proposed as a mechanism for two-dimensional melting [39,40]. The free energy of low angle grain boundaries (LAGBs) changes sign at the Kosterlitz-Thouless melting temperature [41]. However, much less is known about their statistical mechanics at lower temperatures, particularly in the presence of a periodic Peierls pinning potential. In this work, we study the statistical mechanics of LAGBs embedded in a host 2D crystal. Although LAGBs may not be an equilibrium feature of crystals with rectangular boundary conditions, they appear in the ground state of flat crystals with, e.g., trapezoidal boundary conditions. See Fig. 1(a), where a crystal with length  $L$  and width  $W$  is trapped between slanted walls, as could be studied in both experiments and simulations. When  $W \sim L \gg a$ , it is straightforward to show that a grain boundary is preferred over a strained defect-free crystal (see Supplemental Material [42]). We model the LAGB as a one-dimensional array of dislocations, with identical

Burgers vectors directed perpendicular to the boundary, embedded in a 2D continuous elastic medium. “Low angle” means dislocation spacings large enough so that these defects are well defined, with glide planes approximately perpendicular to the interface itself. We also assume a periodic Peierls potential transverse to the boundary itself [47] (Fig. 1). Mapping onto a model of quantum Brownian motion in imaginary time [48] allows a renormalization group treatment of the depinning transition. By analytically calculating dislocation correlations in various regimes, and numerically testing our theory using a mapping onto random matrix theory, we uncover the phase diagram in Fig. 2(a). The sharp one-dimensional phase transitions displayed in Fig. 2(a) are only possible because of the long range interactions between dislocations in the LAGB. Note that the transitions in Eqs. (5) and (17) below can also be expressed in terms of a dimensionless temperature  $\Gamma \equiv k_B T / Y b^2$ , and so the transitions can also be realized by tuning the interaction strength instead of  $k_B T$ .

At low temperatures, the LAGB is in a pinned phase, with dislocations localized along their glide directions by Peierls potential. Upon increasing the temperature, we find a depinning transition at  $T = T_p$ ; above which, the Peierls potential is overcome by thermal fluctuations and the transverse LAGB fluctuations grow logarithmically with distance along the boundary. As the temperature

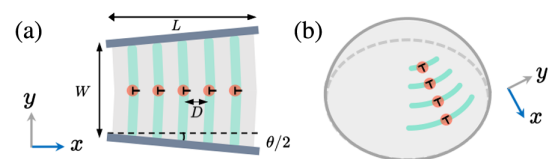


FIG. 1. Schematic of a single LAGB consisting of point dislocations (orange) with Burgers vectors aligned along their glide planes (turquoise) and embedded (a) in a flat 2D crystal with wedge angle  $\theta$  and (b) in a curved 2D crystal.

continues to increase, the quasi-long range ordered depinned LAGB melts via a series of phase transitions at  $\{T_c^{(m)}\}$ , marked by the sequential disappearance of power law divergences at ever-smaller Bragg peaks  $\{G_m\}$ . These transitions proceed until only the final peak at  $G_1$  remains; after which, the LAGB melts with the host crystal, if the host crystal has not already melted by some other mechanism (see, e.g., Ref. [49] and references therein).

Equilibrium configurations of symmetric grain boundaries in  $d = 2$ , without shear load, can be modeled by pointlike edge dislocations with glide planes perpendicular to the boundary [Fig. 1(a)]. Note that LAGBs can also arise on curved 2D crystals [50–52], where grain boundary scars form to relieve the excess strain introduced by Gaussian curvature and associated topological defects such as disclinations [34,52] [Fig. 1(b)].

The energy of a LAGB, consisting of  $N$  point edge dislocations, embedded in a 2D crystal is [47]

$$H[\{x_n, y_n\}] = -\frac{Yb^2}{8\pi} \sum_{n \neq m} \left[ \frac{1}{2} \ln |(x_n - x_m)^2 + (y_n - y_m)^2| - \frac{(y_n - y_m)^2}{(x_n - x_m)^2 + (y_n - y_m)^2} \right] - V_{\text{Peierls}} \sum_n \cos\left(\frac{2\pi y_n}{a}\right), \quad (1)$$

where the LAGB is oriented along  $\hat{x}$ ,  $b$  is the magnitude of the Burgers vector along  $\hat{y}$  (assumed equal to the lattice constant  $a$  for simplicity), and  $Y = 4\mu(\mu + \lambda)/(2\mu + \lambda)$  is the 2D Young's modulus, where  $\mu$  and  $\lambda$  are the Lamé coefficients. The position of the  $n$ th dislocation is given by  $(x_n, y_n) = (nD + u_n^{(x)}, u_n^{(y)})$ , where  $u_n^{(x)}$  and  $u_n^{(y)}$  are the longitudinal and transverse displacements of these defects due to thermal fluctuations. Their equilibrium positions are aligned at  $y = 0$  to balance the Peach-Kohler force due to interactions with other dislocations, and they are evenly spaced along  $\hat{x}$  with an average spacing  $D$  [31,32,47]. We assume that both glide and climb displacements are in thermal equilibrium, as could be achieved by having a 2D host crystal coexisting with a three-dimensional (3D) vapor phase, which effectively supplies a reservoir of vacancies and interstitial defects.

Provided that  $T$  is not too close to the melting temperature  $T_m$  of the host crystal, we expect that typical displacement differences are much smaller than the dislocation separations:  $|u_n - u_m| \ll |n - m|D$ . Upon expanding to quadratic order in the transverse glide displacements  $\{u_n^{(y)}\}$ , we obtain [31,32,40]

$$H = \frac{Yb^2}{8D^2} \int \frac{dq_x}{2\pi} |q_x| |u^{(y)}(q_x)|^2 - V_{\text{Peierls}} \sum_n \cos\left(\frac{2\pi u_n^{(y)}}{a}\right) - \frac{Yb^2}{8\pi} \sum_{n \neq m} \ln |D(n - m) + (u_n^{(x)} - u_m^{(x)})|. \quad (2)$$

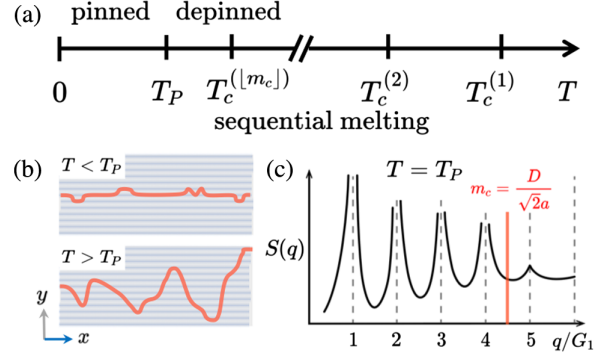


FIG. 2. (a) Phase diagram of a LAGB embedded in a 2D crystal. (b) Schematic of a LAGB below and above the depinning transition, with transverse grain boundary correlations given by Eqs. (6) and (7). Gray lines illustrate transverse Peierls potential. (c) Schematic of the structure factor ( $q \equiv q_x$ ) at the depinning transition with power law divergences in Bragg peaks according to Eq. (14) at  $\{G_m\}$ , provided the Bragg peak index  $m < m_c$  [Eq. (16)].

The first term, representing long range interactions, has been written in Fourier space.

*Thermal depinning.*—We first examine the behavior of glide fluctuations transverse to the boundary. Upon integrating out the longitudinal  $\{u_n^{(x)}\}$  degrees of freedom, the fluctuation energy for the remaining transverse modes becomes

$$H_t = \frac{Yb^2}{8D^2} \int \frac{dq_x}{2\pi} |q_x| |u^{(y)}(q_x)|^2 - V_{\text{Peierls}} \sum_n \cos\left(\frac{2\pi u_n^{(y)}}{a}\right). \quad (3)$$

A similar Hamiltonian was proposed to model dislocations in a zipperlike interface [53]. In that case, however, the Peierls potential acts *along* the boundary rather than perpendicular to it. The reduced Hamiltonian of Eq. (3) maps exactly onto the action of a quantum Brownian particle in a periodic potential in imaginary time [48,54,55]. The repulsive logarithmic interaction between dislocations maps onto a friction force that resists the quantum particle tunneling between minima in the periodic potential. The renormalization group recursion relation for the scale-dependent Peierls potential  $V_{\text{Peierls}}(l)$  reads [48,54]

$$\frac{dV_{\text{Peierls}}(l)}{dl} = \left(1 - \frac{1}{\gamma}\right) V_{\text{Peierls}}(l), \quad (4)$$

and it predicts a delocalization transition for the LAGB. Here,

$$\gamma = \frac{1}{k_B T} \frac{Y b^2 a^2}{8\pi D^2},$$

where  $a = b$  is the lattice constant of the host crystal, and we obtain the depinning temperature  $T_P$  as

$$k_B T_P = \theta^2 \frac{Y b^2}{8\pi}, \quad (5)$$

where  $\theta = a/D$  is the usual misorientation angle of a symmetric LAGB [47].

As illustrated in Fig. 2(b), below the depinning transition  $T < T_P$ , the LAGB dislocations are locked close to a particular minimum of the Peierls potential, even in the presence of thermal fluctuations, and the spatial correlation function of the displacements is constant for large separation distances,

$$\lim_{x \rightarrow \infty} \langle |u^{(y)}(x) - u^{(y)}(0)|^2 \rangle = \left( \frac{a}{2\pi} \right)^2 \frac{k_B T}{V_{\text{Peierls}}}. \quad (6)$$

For  $T > T_P$ , the Peierls potential can be neglected at large distances, and the spatial correlation function of the depinned dislocation displacements grows logarithmically with the separation distances  $x$  along the LAGB:

$$\lim_{x \rightarrow \infty} \langle |u^{(y)}(x) - u^{(y)}(0)|^2 \rangle \approx \frac{8 k_B T D^2}{\pi Y b^2} \ln(x). \quad (7)$$

Although this behavior is reminiscent of roughened 2D interfaces [56–58], typical roughened one-dimensional (1D) interfaces with *short* range interactions, in fact, have fluctuations that grow as  $\sqrt{x}$ .

When  $T \rightarrow T_P^+$ , we obtain the following universal scaling relation using Eqs. (5) and (7):

$$\frac{\lim_{x \rightarrow \infty} \langle |u^{(y)}(x) - u^{(y)}(0)|^2 \rangle}{\ln(x)} = \frac{a^2}{\pi^2}. \quad (8)$$

*Melting.*—To study the melting of longitudinal LAGB order, we now focus on the climb degrees of freedom and examine the 1D structure factor as a function of momenta  $q_x$  near the reciprocal lattice vectors  $\{G_m = 2\pi m/D\}$ . Both above and below the depinning transition  $T = T_P$ , we can integrate out the transverse degrees of freedom  $\{u_n^{(y)}\}$  from the dislocation partition function associated with Eq. (1), and we obtain an effective nonlinear energy for the longitudinal coordinates  $\{x_n\}$  along the boundary,

$$H_\ell(\{x_n\}) = -\frac{Y b^2}{8\pi} \sum_{n \neq m} \ln |x_n - x_m|. \quad (9)$$

{Neglected terms of  $O[(u_n^{(x)})^2 (u_n^{(y)})^2]$  do not affect the coefficient of the logarithm within perturbation theory.} On

denoting  $q \equiv q_x$ , setting  $x_n = Dn + u_n^{(x)}$ , and expanding to quadratic order in longitudinal displacements, Eq. (9) in momentum space becomes ( $q_x \equiv q$ ) [40]:

$$H = \frac{Y b^2}{8D^2} \int \frac{dq}{2\pi} |q| |u^{(x)}(q)|^2. \quad (10)$$

We can now compute the asymptotic forms of the structure factor  $S(q) = \langle |\rho(q)|^2 \rangle / N$ , where

$$\rho(q) = \sum_n e^{iqx_n},$$

in both the  $q \rightarrow 0$  and  $q \rightarrow G_m$  limits. When  $q \rightarrow 0$ , we can construct a hydrodynamic density fluctuation field  $\delta\rho(x)$  [59]. Upon writing the energy in Eq. (10) in terms of density fluctuations with  $\delta\rho(x) = \rho_0 \partial_x u^{(x)}(x)$ , where  $\rho_0 = \langle \rho(x) \rangle \equiv D^{-1}$  is the average dislocation density, we obtain from Eq. (10)

$$\lim_{q \rightarrow 0} S(q) \approx \frac{8\pi k_B T}{Y b^2} |\bar{q}|, \quad (11)$$

where  $\bar{q} \equiv q/2\pi/D$  is the dimensionless wave vector. The linear vanishing of  $S(q)$  as  $q \rightarrow 0$  indicates incompressibility associated with dislocations with identical Burgers vectors, similar to a Coulomb gas of like-signed charges.

On now setting  $q = G_m + k$ , with  $k \ll G_m$ , we obtain for the structure factor  $S(q)$  near the reciprocal lattice vectors  $G_m \neq 0$ :

$$S(q \approx G_m) \approx \sum_{s=-\infty}^{\infty} e^{iksD - (G_m^2/2) \langle |u_s^{(x)} - u_0^{(x)}|^2 \rangle}. \quad (12)$$

where we have used the properties of Gaussian thermal averages to evaluate  $\langle \exp[iG_m(u_s^{(x)} - u_0^{(x)})] \rangle$ . On extracting  $\langle u^{(x)}(q) u^{(x)}(q') \rangle$  from Eq. (10) and utilizing the properties of cosine integrals [60], we obtain the displacement correlation  $C(s) \equiv \langle |u_s^{(x)} - u_0^{(x)}|^2 \rangle$  in the limit of large  $s \rightarrow \infty$  as

$$C(s) = \frac{8D^2 k_B T}{\pi Y b^2} \left( \gamma + \ln(\pi s) + O\left[ \frac{\cos(\pi s)}{s} \right] \right), \quad (13)$$

where  $\gamma \approx 0.577$  is the Euler-Mascheroni constant. Upon substituting Eq. (13) into Eq. (12), we obtain the singular behavior of  $S(q)$  near the  $m$ th reciprocal lattice vector  $G_m$  as

$$\lim_{q \rightarrow G_m} S(q) \sim \frac{1}{|q - G_m|^{1-\alpha_m(T)}}. \quad (14)$$

where  $1 - \alpha_m(T)$  is a temperature-dependent susceptibility critical exponent,

$$\alpha_m(T) = m^2 \frac{16\pi k_B T}{Yb^2}. \quad (15)$$

Equation (14) predicts that at temperatures low enough such that  $\alpha_m(T) \leq 1$ , the structure factor diverges as  $q$  approaches the  $m$ th reciprocal lattice vector  $q \rightarrow G_m$ , and the higher order Bragg peaks are less divergent than the more prominent ones closer to the origin. These power law Bragg peaks for LAGBs are reminiscent of the Bragg peaks below the melting temperature of 2D point particles [61,62]. They replace the usual Lorentzian peaks expected for conventional one-dimensional crystals without long range order [63], and they are due to long range interactions between the dislocations in the grain boundary.

As illustrated in Fig. 2(c), the Bragg peaks at  $\{G_m\}$  (1) remain finite if  $m$  is larger than a critical value  $m > m_c$ , or (2) diverge as a power law with exponent  $1 - \alpha_m(T)$  if  $m < m_c$ . The critical value  $m_c$  is given by

$$m_c = \frac{D}{\sqrt{2}a}. \quad (16)$$

As temperature increases, divergences in higher order Bragg peaks vanish sequentially at a series of transition temperatures  $\{T_c^{(m)}\}$ , where

$$k_B T_c^{(m)} = \frac{1}{m^2} \frac{Yb^2}{16\pi}. \quad (17)$$

The last Bragg peak to disappear is the first-order Bragg peak at  $G_1 = 2\pi/D$ , closest to the origin in momentum space. Interestingly, the temperature at which this last Bragg peak vanishes  $T_c^{(1)}$  seems to coincide with the dislocation pair unbinding temperature of the 2D host crystal, if we neglect screening by bulk dislocation pairs. Note that the dislocation spacing  $D$  drops out in Eqs. (15) and (17) because the  $D$  dependence of the interaction strength in Fourier space of  $\sim 1/D^2$  in Eq. (10) cancels against the  $D$  dependence of the reciprocal lattice vectors  $\{G_m\} = \{2\pi m/D\}$  in Eq. (12).

We also calculate the pair correlations embodied in the radial distribution function  $g(r)$ , which determines the probability of finding a second dislocation a distance  $r$  away from some first existing dislocation. The quantity  $g(r)$  is given by a Fourier transform of the structure factor  $S(q)$  [64]. Since the most prominent Bragg peak at  $G_1$  dominates, we obtain the long distance behavior of  $g(r)$  as

$$\lim_{r \rightarrow \infty} [g(r) - 1] \sim r^{-\alpha_1(T)} \cos(G_1 r). \quad (18)$$

The power law decay of correlations in real space, oscillating on scales of the dislocation spacing  $D$ , are similar to 2D “quasi-long range order” [61,62] but arise here in a 1D system with long range interactions.

*Random matrix simulations.*—We now utilize random matrix theory—the general  $\beta$ -Gaussian (Hermite) ensemble [65]—which can efficiently simulate the long range interactions embodied in Eq. (9) at finite temperatures. We can test quantitatively the predictions of Eqs. (14) and (18) that result from a harmonic approximation to this quantity because the matrix eigenvalues correspond to dislocation positions. The timescale for direct numerical simulations with, say, molecular dynamics for  $N$  particles with long range interactions can be quite large, scaling as  $O(N^{5/2})$  [66]. However, we can obtain an equilibrium configuration of a LAGB at any temperature  $T$  by diagonalizing the following symmetric, tridiagonal random matrix [65] {an operation that scales only as  $O(N \log N)$  [67]}:

$$H_\beta = \frac{1}{\sqrt{2}} \begin{bmatrix} N(0,2) & \chi_{(N-1)\beta} & & & 0 \\ \chi_{(N-1)\beta} & N(0,2) & \chi_{(N-2)\beta} & & \\ & & \ddots & \ddots & \ddots \\ & & & \chi_{2\beta} & N(0,2) & \chi_\beta \\ 0 & & & & \chi_\beta & N(0,2) \end{bmatrix}. \quad (19)$$

In Eq. (19),  $N(0,2)$  indicates a random number drawn from the normal distribution with mean 0 and variance 2,  $\chi_k$  represents a random number drawn from the chi distribution [68], and  $\beta > 0$  can assume any positive value. We can easily tune the temperature of our simulations by changing the random matrix inverse temperature parameter  $\beta$ , i.e., the Dyson index, which is related to the inverse temperature of the LAGB by

$$\beta \equiv \frac{Yb^2}{4\pi} \frac{1}{k_B T}. \quad (20)$$

The eigenvalue density of Eq. (19) follows the Wigner semicircular distribution [65], while the eigenvalue statistics near the center of the spectrum (with an approximately flat density of states) map exactly onto the statistical mechanics of LAGBs (see Supplemental Material for details [42]). Specifically, the joint probability distribution function of the random matrix eigenvalues at the center of the spectrum at a particular value of  $\beta$  is proportional to the dislocation Boltzmann factor  $e^{-(H/k_B T)}$  associated with Eq. (9) for a LAGB at temperature  $T$  corresponding to Eq. (20) [69].

The structure factors  $S(q)$  extracted from random matrix simulations in Fig. 3(a) indeed reveal the sequential disappearance of the power law divergence of the  $m$ th Bragg peaks at the transition temperatures  $\{T_c^{(m)}\}$  predicted by Eq. (17). We also checked that the Bragg peak divergence in  $S(q)$  and the decay of the radial distribution function  $g(r)$  behave according to Eqs. (11), (14), and (18),

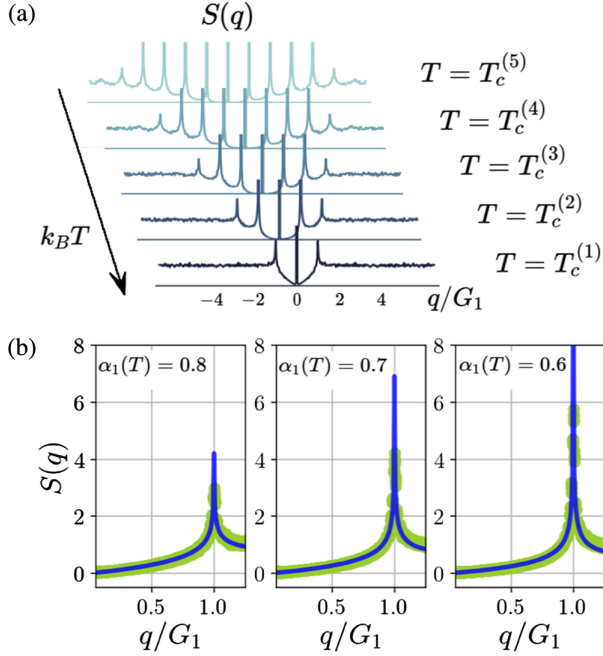


FIG. 3. (a) Structure factors extracted from random matrix simulations (RMSs) at the critical temperatures in Eq. (17) show the sequential disappearance of the algebraic Bragg peak divergence at  $G_m$ . (b) The first-order Bragg peak extracted from RMSs (green) and compared with our theory in Eq. (21) (blue) at three different temperatures given by inverting  $\alpha_1(T)$  in Eq. (15). Theory and RMSs show excellent agreement.

with temperature-dependent exponents given by  $1 - \alpha_m(T)$  and  $\alpha_m(T)$ , respectively.

We can also utilize results from random matrix theory for *standard* Gaussian ensembles [70] to conjecture exact asymptotic expressions for  $S(q)$  near the first Bragg peak in the temperature range  $T_c^{(2)} < T \leq T_c^{(1)}$ . Upon combining the scalings embodied in Eqs. (11) and (14), we expect that (see Supplemental Material [42])

$$S(q) \approx \frac{\alpha_1(T)}{2} |\bar{q}| + \left| \frac{\bar{q}}{2} \right|^{\alpha_1(T)} \frac{\alpha_1(T)}{2(1 - \alpha_1(T))} \left[ \frac{1}{(1 - \bar{q})^{1 - \alpha_1(T)}} - 1 \right], \quad (21)$$

where  $\bar{q} = q/G_1$ , with analogous results for the radial distribution function. As shown in Fig. 3(b), Eq. (21) shows excellent agreement with results from random matrix simulations.

We note in conclusion that in the absence of a coexisting 3D vapor, dislocation climb out of the glide plane can be frozen out at temperatures far below the melting transition of the host crystal,  $T \ll T_m$  [31]. The thermal depinning transition associated with the transverse dislocation glide modes nevertheless occurs as described above. Above the depinning transition, as temperature increases, dislocation climb will be increasingly facilitated by dislocations created and annihilated via glide motion to and from the

boundaries of the host crystal and by the proliferation of dislocation pairs near the melting of the host lattice [40,41]. Although the LAGB structure factor might approximate delta function Bragg peaks when  $T \ll T_m$  as climb is forbidden, we expect a gradual crossover to algebraic Bragg peaks at higher temperatures such that  $T \gtrsim T_P$ . Phase field methods [30,71] might be a particularly efficient way of testing our results via simulations.

In the future, we hope to obtain a similar understanding of the statistical mechanics of both grain boundaries and dislocation pileups subject to a Peierls potential in three dimensions [20,31] and two-dimensional materials that allow out-of-plane deformations [72].

We are grateful for helpful conversations with F. Spaepen and J. Huang. G. H. Z. acknowledges support by the Paul and Daisy Soros Fellowship and the National Science Foundation Graduate Research Fellowship under Grant No. DGE1745303. This work was also supported by the NSF through the Harvard Materials Science and Engineering Center, via Grant No. DMR-2011754, as well as by Grant No. DMR-1608501.

- [1] G. Gottstein and L. S. Shvindlerman, *Grain Boundary Migration in Metals: Thermodynamics, Kinetics, Applications* (CRC Press, Boca Raton, 2009).
- [2] R. W. Balluffi and A. P. Sutton, *Interfaces in Crystalline Materials* (Clarendon, Oxford, 2006).
- [3] P. R. Cantwell, M. Tang, S. J. Dillon, J. Luo, G. S. Rohrer, and M. P. Harmer, *Acta Mater.* **62**, 1 (2014).
- [4] E. A. Holm and S. M. Foiles, *Science* **328**, 1138 (2010).
- [5] D. L. Olmsted, S. M. Foiles, and E. A. Holm, *Scr. Mater.* **57**, 1161 (2007).
- [6] L. Lu, M. Sui, and K. Lu, *Science* **287**, 1463 (2000).
- [7] J. Broughton and G. Gilmer, *Model. Simul. Mater. Sci. Eng.* **6**, 87 (1998).
- [8] J. W. Cahn, Y. Mishin, and A. Suzuki, *Acta Mater.* **54**, 4953 (2006).
- [9] H. Hilgenkamp and J. Mannhart, *Rev. Mod. Phys.* **74**, 485 (2002).
- [10] T. B. Limbu, K. R. Hahn, F. Mendoza, S. Sahoo, J. J. Razink, R. S. Katiyar, B. R. Weiner, and G. Morell, *Carbon* **2017** 367, 117.
- [11] J. Zhang and J. Zhao, *J. Appl. Phys.* **113**, 043514 (2013).
- [12] O. V. Yazyev and S. G. Louie, *Nat. Mater.* **9**, 806 (2010).
- [13] S. Babcock and J. Vargas, *Annu. Rev. Mater. Sci.* **25**, 193 (1995).
- [14] Q. Yu, L. A. Jauregui, W. Wu, R. Colby, J. Tian, Z. Su, H. Cao, Z. Liu, D. Pandey, D. Wei *et al.*, *Nat. Mater.* **10**, 443 (2011).
- [15] P. Schweizer, C. Dolle, and E. Spiecker, *Sci. Adv.* **4**, eaat4712 (2018).
- [16] C. Rottman, *Phys. Rev. Lett.* **57**, 735 (1986).
- [17] S. Chui, *Europhys. Lett.* **87**, 66001 (2009).
- [18] T. Hsieh and R. Balluffi, *Acta Metall.* **37**, 2133 (1989).
- [19] S. B. Lee, S.-Y. Lee, S. J. Yoo, Y. Kim, J.-G. Kim, M. Kim, and H. N. Han, *Phys. Rev. Mater.* **2**, 113405 (2018).

- [20] M. Liao, X. Xiao, S. T. Chui, and Y. Han, *Phys. Rev. X* **8**, 021045 (2018).
- [21] I. Daruka and J. C. Hamilton, *Phys. Rev. Lett.* **92**, 246105 (2004).
- [22] R. Kikuchi and J. W. Cahn, *Phys. Rev. B* **21**, 1893 (1980).
- [23] A. M. Alsayed, M. F. Islam, J. Zhang, P. J. Collings, and A. G. Yodh, *Science* **309**, 1207 (2005).
- [24] D. L. Olmsted, D. Buta, A. Adland, S. M. Foiles, M. Asta, and A. Karma, *Phys. Rev. Lett.* **106**, 046101 (2011).
- [25] T. Frolov, D. L. Olmsted, M. Asta, and Y. Mishin, *Nat. Commun.* **4**, 1899 (2013).
- [26] B. Li, D. Zhou, and Y. Han, *Nat. Rev. Mater.* **1**, 1 (2016).
- [27] K. Novoselov, A. Mishchenko, A. Carvalho, and A. C. Neto, *Science* **353**, aac9439 (2016).
- [28] K. Zhang, Y. Feng, F. Wang, Z. Yang, and J. Wang, *J. Mater. Chem. C* **5**, 11992 (2017).
- [29] A. M. Van Der Zande, P. Y. Huang, D. A. Chenet, T. C. Berkelbach, Y. You, G.-H. Lee, T. F. Heinz, D. R. Reichman, D. A. Muller, and J. C. Hone, *Nat. Mater.* **12**, 554 (2013).
- [30] J. Mellenthin, A. Karma, and M. Plapp, *Phys. Rev. B* **78**, 184110 (2008).
- [31] P. Moretti, M. Carmen Miguel, M. Zaiser, and S. Zapperi, *Phys. Rev. B* **69**, 214103 (2004).
- [32] F. Leoni and S. Zapperi, *J. Stat. Mech.* (2007) P12004.
- [33] P. Lipowsky, M. J. Bowick, J. H. Meinke, D. R. Nelson, and A. R. Bausch, *Nat. Mater.* **4**, 407 (2005).
- [34] A. Bausch, M. J. Bowick, A. Cacciuto, A. Dinsmore, M. Hsu, D. Nelson, M. Nikolaides, A. Travesset, and D. Weitz, *Science* **299**, 1716 (2003).
- [35] T. O. E. Skinner, D. G. A. L. Aarts, and R. P. A. Dullens, *Phys. Rev. Lett.* **105**, 168301 (2010).
- [36] P. Y. Huang, C. S. Ruiz-Vargas, A. M. Van Der Zande, W. S. Whitney, M. P. Levendorf, J. W. Kevek, S. Garg, J. S. Alden, C. J. Hustedt, Y. Zhu *et al.*, *Nature (London)* **469**, 389 (2011).
- [37] K. Kim, Z. Lee, W. Regan, C. Kisielowski, M. Crommie, and A. Zettl, *ACS Nano* **5**, 2142 (2011).
- [38] A. L. Gibb, N. Alem, J.-H. Chen, K. J. Erickson, J. Ciston, A. Gautam, M. Linck, and A. Zettl, *J. Am. Chem. Soc.* **135**, 6758 (2013).
- [39] S. Chui, *Phys. Rev. Lett.* **48**, 933 (1982).
- [40] S. Chui, *Phys. Rev. B* **28**, 178 (1983).
- [41] D. S. Fisher, B. I. Halperin, and R. Morf, *Phys. Rev. B* **20**, 4692 (1979).
- [42] See Supplemental Material at <http://link.aps.org/supplemental/10.1103/PhysRevLett.125.215503> for details on ground state calculations with alternative boundary conditions, random matrix mapping, and derivation of asymptotic expressions for the structure factor, which includes Refs. [43–46].
- [43] J. M. Kosterlitz, *Rev. Mod. Phys.* **89**, 040501 (2017).
- [44] E. P. Wigner, *Ann. Math.* **67**, 325 (1958).
- [45] G. Livan, M. Novaes, and P. Vivo, *Introduction to Random Matrices: Theory and Practice* (Springer, New York, 2018), Vol. 26.
- [46] G. H. Zhang and D. R. Nelson, [arXiv:2009.14402](https://arxiv.org/abs/2009.14402).
- [47] J. P. Hirth and J. Lothe, *Theory of Dislocations* (McGraw-Hill, New York, 1983).
- [48] M. P. A. Fisher and W. Zwerger, *Phys. Rev. B* **32**, 6190 (1985).
- [49] Y.-W. Li and M. P. Ciamarra, *Phys. Rev. Lett.* **124**, 218002 (2020).
- [50] A. Azadi and G. M. Grason, *Phys. Rev. Lett.* **112**, 225502 (2014).
- [51] A. Azadi and G. M. Grason, *Phys. Rev. E* **94**, 013003 (2016).
- [52] M. J. Bowick, D. R. Nelson, and A. Travesset, *Phys. Rev. B* **62**, 8738 (2000).
- [53] E. B. Kolomeisky and J. P. Straley, *Phys. Rev. Lett.* **76**, 2930 (1996).
- [54] A. J. Leggett, S. Chakravarty, A. T. Dorsey, M. P. Fisher, A. Garg, and W. Zwerger, *Rev. Mod. Phys.* **59**, 1 (1987).
- [55] G. H. Zhang, *Phys. Rev. B* **96**, 205440 (2017).
- [56] M. Kardar, *Statistical Physics of Fields* (Cambridge University Press, Cambridge, England, 2007).
- [57] S. Chui and J. Weeks, *Phys. Rev. B* **14**, 4978 (1976).
- [58] T. Ohta and D. Jasnow, *Phys. Rev. B* **20**, 139 (1979).
- [59] D. R. Nelson, *Defects and Geometry in Condensed Matter Physics* (Cambridge University Press, Cambridge, England, 2002).
- [60] F. W. Olver, D. W. Lozier, R. F. Boisvert, and C. W. Clark, *NIST Handbook of Mathematical Functions* (Cambridge University Press, Cambridge, England, 2010).
- [61] D. R. Nelson and B. I. Halperin, *Phys. Rev. B* **19**, 2457 (1979).
- [62] B. I. Halperin and D. R. Nelson, *Phys. Rev. Lett.* **41**, 121 (1978).
- [63] V. J. Emery and J. D. Axe, *Phys. Rev. Lett.* **40**, 1507 (1978).
- [64] R. K. Pathria and P. D. Beale, *Statistical Mechanics* (Elsevier, Amsterdam, 2011).
- [65] I. Dumitriu and A. Edelman, *J. Math. Phys. (N.Y.)* **43**, 5830 (2002).
- [66] With long range interactions, all  $N$  particles must be updated for each of the  $N$  equations of motion, and so the computational effort scales as  $\sim N^2\tau$ . The timescale  $\tau$  to achieve equilibrium is inversely proportional to the frequency of longest wavelength longitudinal phonon modes  $\tau^{-1} \sim \omega(q) \sim q^{1/2} > \sim N^{-1/2}$ , giving an equilibration time that scales like  $N^{5/2}$ .
- [67] E. S. Coakley and V. Rokhlin, *Appl. Comput. Harmon. Anal.* **34**, 379 (2013).
- [68] N. L. Johnson, S. Kotz, and N. Balakrishnan, *Continuous Univariate Distributions* (John Wiley & Sons, New York, 1995).
- [69] Note that we do *not* set  $\beta = 1/k_B T$ , which is the usual notational convention in statistical mechanics.
- [70] M. L. Mehta, *Random Matrices* (Elsevier, New York, 2004).
- [71] K. R. Elder, N. Provatas, J. Berry, P. Stefanovic, and M. Grant, *Phys. Rev. B* **75**, 064107 (2007).
- [72] O. V. Yazyev and S. G. Louie, *Phys. Rev. B* **81**, 195420 (2010).